J. of Supercritical Fluids 55 (2010) 455–461

Contents lists available at ScienceDirect

The Journal of Supercritical Fluids

journal homepage: www.elsevier.com/locate/supflu

Critical behavior of pure confined fluids from an extension of the van der Waals equation of state

Leonardo Travalloni[a], Marcelo Castier[b,*], Frederico W. Tavares[a], Stanley I. Sandler[c]

[a] Escola de Química, Universidade Federal do Rio de Janeiro, C.P. 68542, CEP 21949-900, Rio de Janeiro, RJ, Brazil
[b] Department of Chemical and Petroleum Engineering, United Arab Emirates University, P.O. Box 17555, Al Ain, United Arab Emirates
[c] Department of Chemical Engineering, University of Delaware, 19716-3110, Newark, DE, USA

ARTICLE INFO

Article history:
Received 13 April 2010
Received in revised form
12 September 2010
Accepted 15 September 2010

Keywords:
Confined fluid
State equation
Critical point
Adsorption

ABSTRACT

The critical behavior of pure fluids confined in porous solids is investigated using an extension of the van der Waals equation of state. The effects of pore size and of the interaction between fluid molecules and pore walls are evaluated. Fluid molecules were assumed spherical, interacting with each other and with the walls of cylindrical pores through distinct square-well potentials. It was found that our model may predict either one or two mechanically stable critical points for the confined fluid, depending on its specifications. When two critical points are predicted, one is attributed to a major contribution of molecule–molecule interactions and the other to a major contribution of molecule–wall interactions. The confined fluid critical point(s) presented a complex dependence on the pore size, due to the interplay of molecule–molecule and molecule–wall interactions. It is shown that the prediction of two critical points for confined fluids is useful to describe adsorption isotherms with two phase transitions.

1. Introduction

The thermodynamic behavior of fluids confined in porous media is a subject of fundamental importance to many industrial applications, such as oil extraction, separation processes, and heterogeneous catalysis. In particular, the knowledge of the equilibrium phase behavior and the critical properties of confined fluids is required for the design and optimization of such processes. Confinement changes the fluid behavior due to the geometric constraint of the fluid molecules and the interaction of these molecules with the pore walls (the molecule–wall interaction). Experimental results suggest that a confined fluid has a depressed critical temperature and an increased critical density compared to its bulk properties [1–4]. Moreover, some results indicate that the critical temperature shift increases linearly with inverse pore size [5,6].

The effect of confinement on the fluid critical properties has also been investigated by theory and molecular simulation, giving rise to several interesting predicted behaviors. The linear relation between the critical temperature shift and the inverse pore size was corroborated by both lattice gas modeling and molecular simulation [7], but nonlinear relations have also been observed in recent simulations [8–10]. Theoretical and simulation results for the confined fluid critical density suggest that it increases under confinement in attractive pores, but the inverse occurs in purely repulsive pores [11–14]. However, nonmonotonic relations between the critical density and the pore size have been found for both pore types [7,9,10]. The dependence of the confined fluid critical point on the strength of the molecule–wall interaction has also been studied. There are recent reports of a nonmonotonic behavior for the critical temperature, with a maximum at an intermediate value of the molecule–wall interaction strength, while the critical density seems to increase monotonically with this strength [15–17].

Some authors have focused on developing analytical equation of state models in the attempt to describe the thermodynamic behavior of confined fluids with low computational effort [18–23]. Extensions of the van der Waals equation of state to confined fluids have been shown to predict the critical temperature reduction with pore size reduction either qualitatively [18,22] or quantitatively [20], and a positive shift in the critical density could be predicted with this approach [22]. In our previous work [23], the van der Waals equation of state was extended to confined fluids based on the generalized van der Waals theory [24,25]. It has been found that the proposed model is able to describe different types of adsorption isotherms and to correlate experimental data of pure fluid adsorption quite well. In this work, the critical behavior of pure confined fluids as predicted by this model is investigated. The effects of pore size and of the intensity of the molecule–wall interaction are evaluated.

* Corresponding author. Currently at: Texas A&M University at Qatar, on leave from the Federal University of Rio de Janeiro, Brazil. Tel.: +974 44230534; fax: +974 44230065.
E-mail address: marcelo.castier@qatar.tamu.edu (M. Castier).

0896-8446/$ – see front matter © 2010 Elsevier B.V. All rights reserved.
doi:10.1016/j.supflu.2010.09.008

Nomenclature

a	energy parameter of the van der Waals equation of state for bulk fluids
a_p	van der Waals energy parameter modified by confinement
b	volume parameter of the van der Waals equation of state for bulk fluids
b_p	van der Waals volume parameter modified by confinement
F_{pr}	geometric function in the equation of state for confined fluids
k	Boltzmann constant
N_{av}	Avogadro number
P	pressure
r_p	pore radius
R	ideal gas constant
T	temperature
v	molar volume

Greek letters

δ_p	range parameter of the attractive interaction between a fluid molecule and the pore wall
ε_p	energy parameter of the attractive interaction between a fluid molecule and the pore wall
θ	geometric function in the equation of state for confined fluids
λ	de Broglie wavelength
μ	chemical potential
μ_0	reference chemical potential
ρ	molar density
$\rho_{\max}$	molecular density of the packed fluid modified by confinement
σ	effective diameter of the fluid molecule

Subscripts

a	adsorbed phase
b	bulk phase
c	critical condition
cr	reduced critical condition with respect to the bulk critical condition

2. Model for pure confined fluids

An equation of state model was formulated to describe a fluid confined in a porous medium as a global phase. In model development, it was assumed that the fluid molecules are spheres interacting with each other through the square-well potential, which is consistent with the theoretical basis of the van der Waals equation of state. The confining pores were assumed to be cylinders with continuous and homogeneous walls that interact with the fluid molecules through another square-well potential (this potential function was chosen in order to make the analytical derivation of the model easier). Pairwise additivity was assumed for the attractive parts of both interaction potentials. To compute the attractive contributions to the model, the molecule–wall interaction potential defines three regions inside each pore, as shown in Fig. 1, where δ_p is the square-well width of this potential and σ is the fluid molecule diameter. A geometric constraint was proposed to account for the reduction in the molecule–molecule coordination number due to confinement of the fluid.

A detailed description of the model formulation is presented elsewhere [23]. The equation of state for the confined fluid was obtained from the partial derivative of the canonical partition function of the system with respect to its total volume, maintaining constant the pore radius. Consequently, the infinitesimal change of volume is in the axial direction of the pore, i.e., the axial component of the pressure tensor was obtained. Therefore, the proposed equation of state describes a homogeneous phase in equilibrium along the pore axis, whose properties represent averages over the radial direction. The expressions for the equation of state and the chemical potential of the confined fluid are:

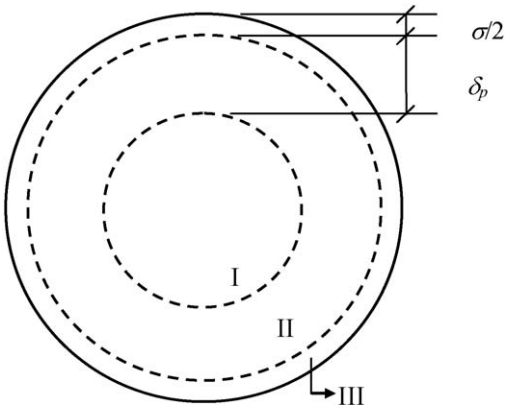

Fig. 1. Regions inside a cylindrical pore, defined by the molecule–wall interaction potential as a function of the distance from the wall.

$$P = \frac{RT}{v - b_p} - \frac{a_p}{v^2} - \theta\frac{b_p}{v^2}\left(1 - \frac{b_p}{v}\right)^{\theta-1}(1 - F_{pr}) \times \left(RT\left(1 - \exp\left(-\frac{N_{av}\varepsilon_p}{RT}\right)\right) - N_{av}\varepsilon_p\right) \quad (1)$$

$$\mu = \mu_0 + RT\left(\ln\left(\frac{N_{av}\lambda^3}{v - b_p}\right) + \left(\frac{b_p}{v - b_p}\right)\right) - \frac{2a_p}{v} - F_{pr}N_{av}\varepsilon_p + \left(1 - (\theta + 1)\frac{b_p}{v}\right)\left(1 - \frac{b_p}{v}\right)^{\theta-1}(1 - F_{pr}) \times \left(RT\left(1 - \exp\left(-\frac{N_{av}\varepsilon_p}{RT}\right)\right) - N_{av}\varepsilon_p\right) \quad (2)$$

where P, T, v, and μ are the pressure, the temperature, the molar volume, and the chemical potential of the fluid inside each pore, respectively, R is the ideal gas constant, N_{av} is the Avogadro number, ε_p is the energy parameter of the molecule–wall interaction, μ_0 is the reference chemical potential, λ is the de Broglie wavelength, F_{pr} and θ are geometric functions given by:

$$F_{pr} = \frac{(r_p - \sigma/2)^2 - (r_p - \sigma/2 - \delta_p)^2}{(r_p - \sigma/2)^2} \quad (3)$$

$$\theta = \frac{r_p}{\delta_p + \sigma/2} \quad (4)$$

and a_p and b_p are the van der Waals equation of state parameters modified by confinement:

$$a_p = a\left(1 - \frac{2}{5}\frac{\sigma}{r_p}\right) \quad (5)$$

$$b_p = \frac{N_{av}}{\rho_{\max}} \quad (6)$$

In Eqs. (3)–(6), r_p is the pore radius, a is the energy parameter of the original van der Waals equation of state, and $\rho_{\max}$ is the molecular density of the packed fluid, which is a function of the pore size. This functional dependence was modeled based on literature

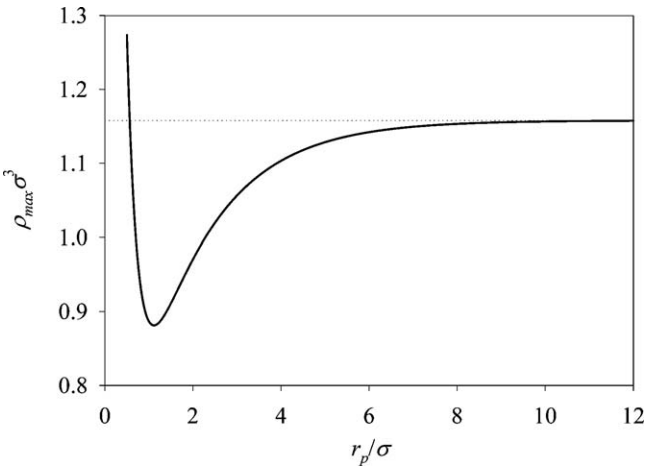

Fig. 2. Variation of the packed fluid dimensionless density with pore size as predicted by Eq. (7).

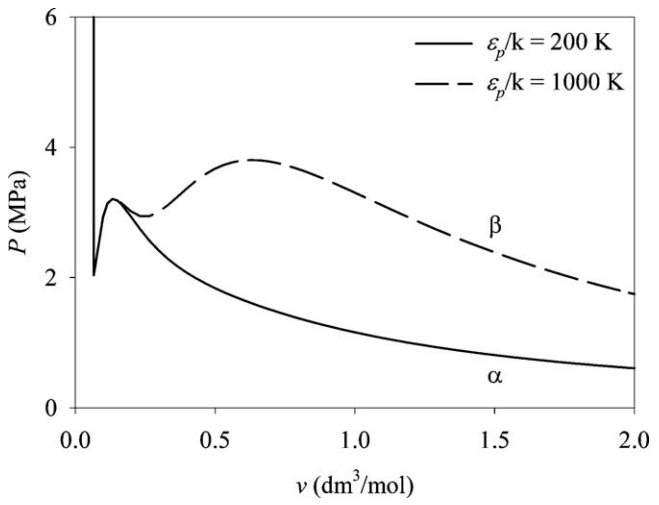

Fig. 3. *P vs. v* isotherms for pure N_2 at 113.58 K confined in a pore with r_p = 19.33 nm (r_p/σ = 50), δ_p/σ = 0.5, and different values of parameter ε_p.

data for the packing of hard spheres in cylinders [26], fitted by the following empirical expression:

$$\rho_{\max}\sigma^3 = c_1 - c_2 \exp\left(c_3\left(0.5 - \frac{r_p}{\sigma}\right)\right) + c_4 \exp\left(c_5\left(0.5 - \frac{r_p}{\sigma}\right)\right) \quad (7)$$

where c_1 = 1.15798, c_2 = 0.479264, c_3 = 0.620861, c_4 = 0.595114, and c_5 = 4.01377. Fig. 2 presents the variation of $\rho_{\max}$ with pore size as predicted by Eq. (7). For consistency between Eq. (7) and the van der Waals equation of state model, the fluid molecule effective diameter is computed from:

$$\sigma = \sqrt[3]{1.15798\frac{b}{N_{av}}} \quad (8)$$

where b is the volume parameter of the original van der Waals equation of state. In this model, the only fitting parameters are the two parameters that characterize the molecule–wall interaction potential (ε_p and δ_p). When $r_p/\sigma \to \infty$ (bulk fluid), Eq. (1) reduces to the van der Waals equation of state. Therefore, this model can describe the average behavior of a fluid from the bulk state to extreme confinement using a single set of parameters for each solid/fluid pair.

3. Critical point calculations

The critical point calculations were carried out using the classical conditions:

$$\begin{cases} (\partial P/\partial v)_{T=T_c} = 0 \\ (\partial^2 P/\partial v^2)_{T=T_c} = 0 \end{cases} \quad (9)$$

The set of Eq. (9) was numerically solved with a modified Newton algorithm using different initial estimates of critical temperature (T_c) and critical volume (v_c) for the confined fluid. The derivatives above were analytically obtained from Eq. (1), as well as the other elements of the Jacobian matrix required by the Newton method: $(\partial^3 P/\partial v^3)_T$, $(\partial^2 P/\partial v\,\partial T)$, and $(\partial^3 P/\partial v^2 \partial T)$. In these calculations, the specifications are the parameters a, b, ε_p, δ_p, and variable r_p. The effects of pore size and of the molecule–wall interaction parameters on the critical behavior of confined nitrogen were evaluated. The bulk parameters (a and b) of pure N_2 were calculated using the conventional formulas of the van der Waals equation of state model as functions of critical temperature and critical volume.

It was found that our model may give either one or three critical points for the confined fluid, depending on its specifications. When three critical points are predicted, only two of them are mechanically stable. Indications of the existence of more than one critical point in confined fluids have been obtained from molecular simulations of Lennard–Jones fluids confined in purely repulsive disordered porous structures [11,14] and from a perturbation theory model of associating fluids confined in hydrophobic slit pores [27]. Also, experimental results suggest that certain pure fluids have two critical points in the bulk state and it was shown that this behavior can be obtained from a fluid model with two repulsive ranges in the molecule–molecule interaction potential [28]. In confined fluids, the repulsive part of the molecule–wall interaction potential could act like a second molecule–molecule repulsion range, resulting in the emergence of a second critical point.

The two possibilities of critical behavior predicted by our model for the confined fluid (one or two stable critical points) can be inferred from Fig. 3, which presents *P vs. v* isotherms for two specifications of parameter ε_p. For the lowest value of ε_p, the isotherm shows a typical subcritical shape (labeled as α), which is associated with a single critical point. For the highest value of ε_p, on the other hand, the isotherm shows an unusual shape (labeled as β), in which there are three regions related to mechanically stable phases (where $\partial P/\partial v < 0$). As the confined fluid temperature is increased from the condition of Fig. 3, it eventually exceeds a critical value and the type-β isotherm assumes the typical subcritical shape, with only one phase transition region. A further increase in temperature results in a typical supercritical isotherm. Therefore, the type-β isotherm is associated with two stable critical points. Besides these critical points, the type-β isotherm is associated with a mechanically unstable critical point, which is related to a virtual transition between the two unstable phases (where $\partial P/\partial v > 0$). In the critical point calculations, the unstable critical point was identified as the one that gives $\partial^3 P/\partial v^3 > 0$ [29].

In what follows, we present the effects of pore size and of the molecule–wall interaction parameters on the stable critical point(s) calculated for the confined fluid. T_{cr} and ρ_{cr} are the reduced critical temperature and density, respectively, scaled with respect to the bulk critical properties of N_2, which are 126.2 K and 11.10 kg mol/m^3 [30]. Figs. 4–7 show the variation of the confined fluid critical points with r_p and ε_p, for δ_p/σ = 0.5. For low ε_p values (Figs. 4 and 5), only one critical point is predicted for each pore size, defining unique critical lines that tend to the bulk critical point when $r_p/\sigma \to \infty$, as expected.

When ε_p = 0, only the repulsive effect of confinement is present, resulting in the monotonic reduction of the critical temperature with the reduction of r_p (Fig. 4). For maximum confinement

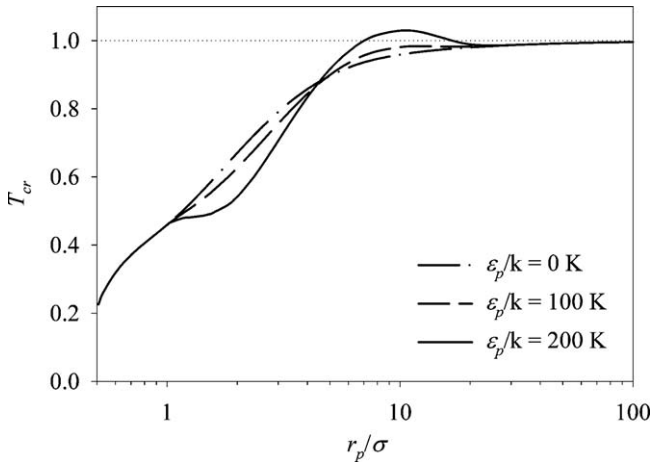

Fig. 4. Reduced critical temperatures of confined N_2 for $\delta_p/\sigma = 0.5$ and low values of parameter ε_p.

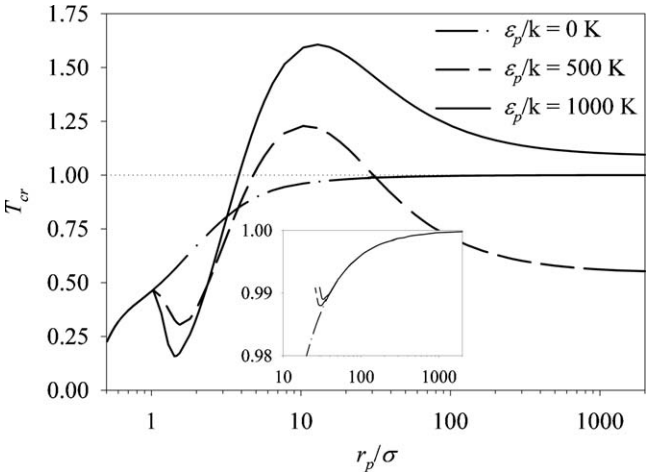

Fig. 6. Reduced critical temperatures of confined N_2 for $\delta_p/\sigma = 0.5$ and higher values of parameter ε_p (the inset is a zoom view of the incomplete T_c lines for the non-zero ε_p values).

($r_p/\sigma = 0.5$), however, it seems that our model does not satisfy the expected limit of $T_c = 0$ for the one-dimensional fluid, which cannot undergo first-order phase transitions [31]. When ε_p is a low non-zero value, the critical line deviates from that of null ε_p only for small pores, in which the attractive effect of confinement is more significant. Around $r_p/\sigma = 10$, the increase of ε_p results in the increase of T_c due to the increasing attractive effect. However, the increase of ε_p also results in the reduction of T_c for r_p/σ between 1 and about 5. This behavior is due to a high geometric constraint hindering the confined phase transition, as suggested by the depression of the fluid packing density in the same r_p range (see Fig. 2). The increase of ε_p results in higher densities for both coexisting confined phases; however, in the aforementioned r_p range this effect is less pronounced for the denser phase, which is closer to the packing limit. Therefore, the density difference between the coexisting confined phases is reduced, leading to the local reduction of T_c with the increase of ε_p.

For null ε_p, the ρ_c line (Fig. 5) follows closely the variation pattern of the packing density with the pore size (Fig. 2). When the molecule–wall attraction is considered, however, the ρ_c line shows an oscillatory behavior that may be related to the interplay of the molecule–molecule attraction, the molecule–wall attraction, and the repulsive effect of confinement. Oscillations of ρ_c with the pore size were also observed from a lattice gas modeling of a Lennard–Jones fluid confined in slit pores [7] and from molecular simulations of a square-well fluid in hard slit pores [9] and of alkanes in attractive slit pores [10].

For high ε_p values (Figs. 6 and 7), one or two critical points may be predicted depending on pore size, defining two critical lines for each value of ε_p. The critical lines shown in the insets for non-zero ε_p values satisfy the bulk limit and present small deviations from the bulk critical point, indicating that they result from a major contribution of molecule–molecule interactions. However, these critical lines vanish below a critical value of r_p (which depends on ε_p), because the contribution of molecule–molecule interactions is overwhelmed by that of molecule–wall interactions. The higher the value of ε_p, the higher is the critical r_p, because the contribution of the molecule–wall interactions predominates even in larger pores. On the other hand, the critical lines shown in full scale are observed in the entire physical range of r_p. These so-called complete critical lines can present large deviations from the bulk critical point, indicating an intense contribution of molecule–wall interactions. Moreover, the complete critical lines for high ε_p values do not satisfy the bulk limit when $r_p/\sigma \to \infty$, as T_c tends to a different limit depending on the value of ε_p. However, the respective critical points collapse to null density when $r_p/\sigma \to \infty$ (Fig. 7). Therefore,

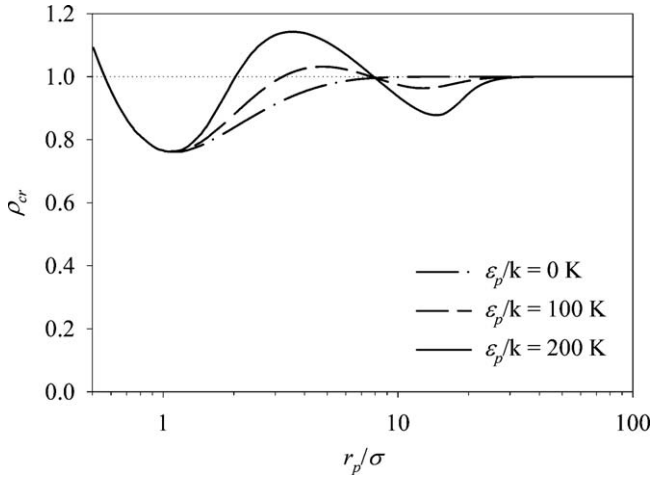

Fig. 5. Reduced critical densities of confined N_2 for $\delta_p/\sigma = 0.5$ and low values of parameter ε_p.

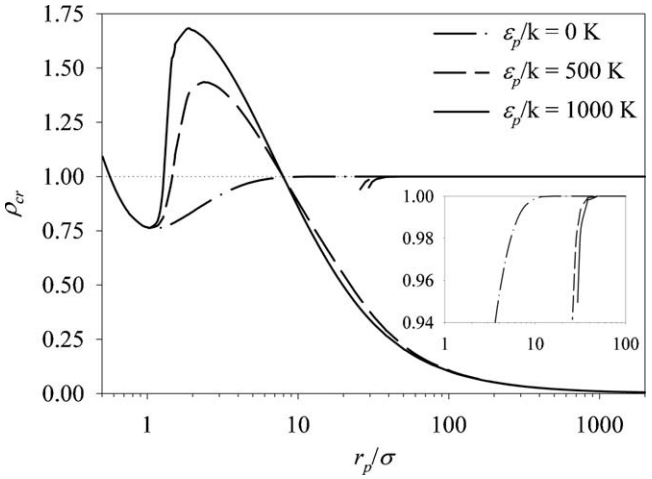

Fig. 7. Reduced critical densities of confined N_2 for $\delta_p/\sigma = 0.5$ and higher values of parameter ε_p (the inset is a zoom view of the incomplete ρ_c lines for the non-zero ε_p values).

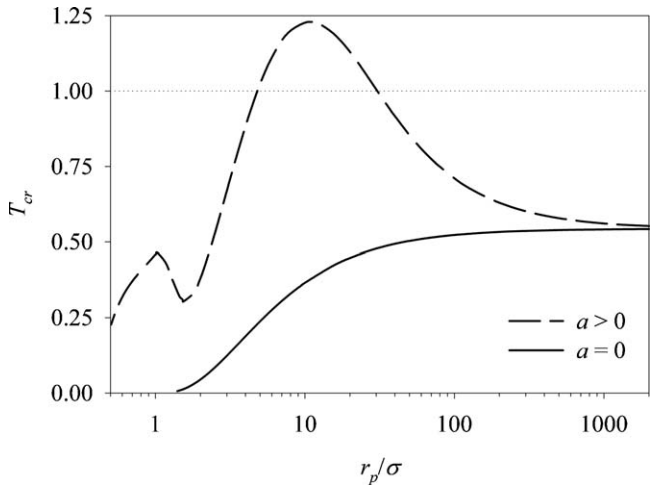

Fig. 8. Reduced critical temperatures of confined N_2 for $\delta_p/\sigma = 0.5$ and $\varepsilon_p/k = 500$ K, with and without molecule–molecule interactions.

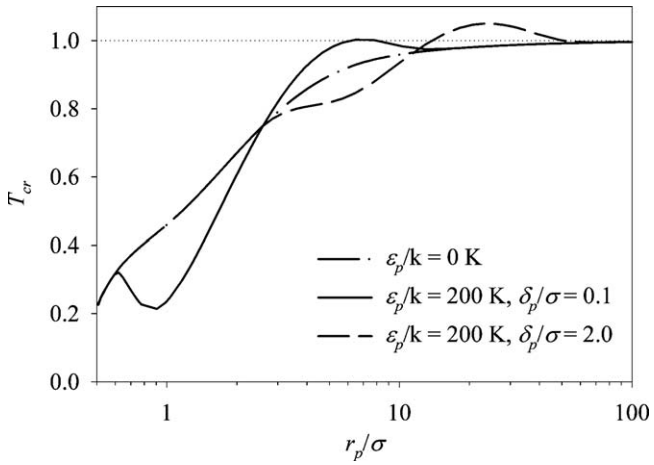

Fig. 10. Reduced critical temperatures of confined N_2 for low values of parameter ε_p and different values of parameter δ_p.

our model predicts only one critical point with physical meaning for the bulk fluid regardless of the value of ε_p, as expected.

At first, it may seem surprising that the complete T_c lines for high ε_p values (Fig. 6) do not satisfy the bulk limit when $r_p/\sigma \to \infty$, since the confinement effect must be negligible in large pores. However, as the pore size increases, the corresponding phase equilibrium is rapidly shifted to lower densities (Fig. 7). At low densities, most of the confined molecules are located near the pore wall, due to its attractive field. Consequently, the attractive effect of confinement remains important in large pores, influencing the critical behavior of the fluid. Figs. 8 and 9 show the complete critical lines for $\delta_p/\sigma = 0.5$ and a relatively high ε_p value, together with the critical lines calculated without accounting for molecule–molecule interactions (i.e., by setting $a = 0$). It can be seen that the bulk limit of the complete critical lines for high ε_p values is a result of the molecule–wall interactions, which agrees with the fact that the corresponding phase equilibrium occurs at low densities, since in this condition the contribution of molecule–molecule interactions is less important. Depending on the strength of the molecule–wall interactions (i.e., depending on the value of ε_p), the bulk limit of the complete T_c lines in Fig. 6 can be lower or higher than the bulk value of T_c.

In Figs. 4–7, the complete critical lines for different ε_p values converge in the range $r_p/\sigma \leq 1$. Note that, for $\delta_p/\sigma = 0.5$, this is the range of r_p in which the whole pore interior is subject to the attractive field of the wall (see Fig. 1). In bulk fluids, the critical point results from a difference in the intensity of attractive molecule–molecule interactions between the two equilibrium phases, which in turn results from the difference in density between the two phases. In a confined fluid, the attractive molecule–wall interactions also contribute to the emergence of a critical point, as shown in Figs. 8 and 9. For $r_p/\sigma \leq 1$, however, the attractive effect of confinement would be the same (per fluid molecule) for two hypothetical phases in equilibrium, regardless of their density difference. Therefore, in that r_p range the critical point is independent of ε_p, changing only with r_p due to the repulsive effect of confinement (i.e., the reduction of the molecule–molecule coordination number).

Figs. 10 and 11 show the variation of the confined fluid critical point with r_p and δ_p, for $\varepsilon_p/k = 200$ K. For this relatively low ε_p value, there is a unique critical line for each δ_p value, since the variation of δ_p does not change the number of critical points calculated for the confined fluid. The number of critical points depends only on pore size and on the value of parameter ε_p, as discussed before. As δ_p increases, the region where the critical lines deviate from that for null ε_p is shifted to higher pore sizes, due to the increase of the attractive effect of confinement. For the same reason, the maximum T_c (Fig. 10) and the critical r_p (for higher ε_p values) increase with δ_p.

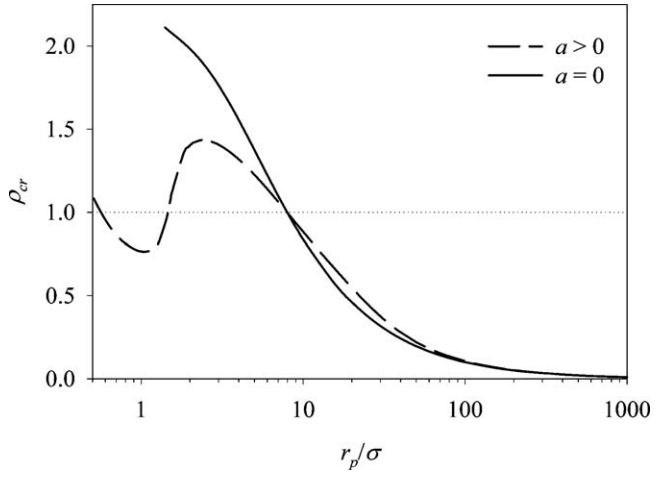

Fig. 9. Reduced critical densities of confined N_2 for $\delta_p/\sigma = 0.5$ and $\varepsilon_p/k = 500$ K, with and without molecule–molecule interactions.

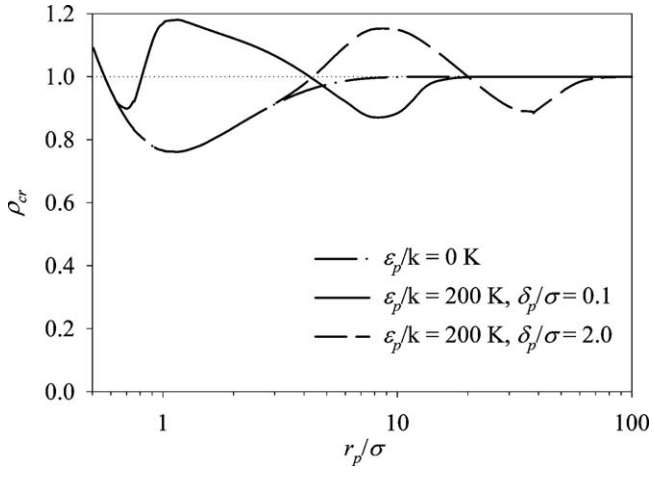

Fig. 11. Reduced critical densities of confined N_2 for low values of parameter ε_p and different values of parameter δ_p.

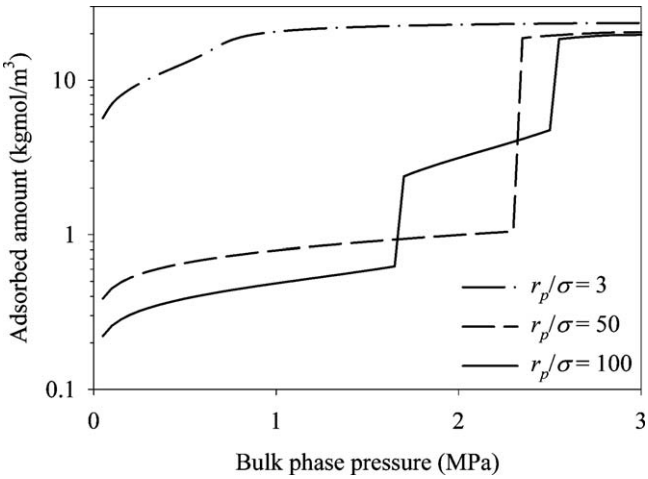

Fig. 12. Adsorption isotherms of N_2 at 113.58 K for $\delta_p/\sigma = 0.5$, $\varepsilon_p/k = 1000$ K, and different pore sizes.

4. Adsorption calculations

A straightforward application of the critical behavior predicted by our model is the description of adsorption isotherms with two phase transitions, related to two different critical points. The adsorption calculations are based on the equilibrium condition:

$$\mu_b(T, P_b; a, b) = \mu_a(T, \rho_a, r_p; a, b, \varepsilon_p, \delta_p) \quad (10)$$

where subscripts a and b denote the adsorbed (confined) and bulk phases, respectively. In these calculations, the specifications are the bulk phase conditions (T, P_b), variable r_p, and parameters a, b, ε_p, and δ_p, allowing the solution of Eq. (10) to find the adsorbed phase density (ρ_a). The methodology for adsorption calculations using our model is detailed elsewhere [23]. However, the methodology described in that work is not entirely appropriate when the confined fluid shows *P vs. v* isotherms of type-β (see Fig. 3). In this case, higher order derivatives of μ_a with respect to ρ_a are required in the adsorption calculation procedure.

Fig. 12 presents adsorption isotherms of N_2 at 113.58 K ($T/T_c = 0.9$, scaling with respect to the bulk value of T_c) calculated for $\delta_p/\sigma = 0.5$, $\varepsilon_p/k = 1000$ K, and different pore sizes. The adsorption profile predicted by our model can show none, one or two phase transitions, depending on the adsorbent pore size (as well as on T and ε_p). For the lowest r_p value, there is only one predicted critical temperature for the confined fluid, which is below the specified adsorption temperature (see Fig. 6). Therefore, the confined fluid is supercritical and the adsorption profile is continuous. A similar profile would be observed if two critical temperatures were predicted below the adsorption temperature. For the highest r_p value, two phase transitions are observed in the adsorption profile because two confined fluid critical temperatures are predicted to occur above the adsorption temperature. As seen in Fig. 6, however, two critical temperatures above the adsorption temperature are also predicted for $r_p/\sigma = 50$, but the corresponding adsorption profile shows only one phase transition, not two. The difference in the adsorption profiles for $r_p/\sigma = 50$ and $r_p/\sigma = 100$ is due to the relative stability behavior of the three possible phases that could occupy the adsorbent pores. Among these phases, the globally stable one is that of highest pressure [23]. For $r_p/\sigma = 100$, each one of the three possible phases is the globally stable one in a particular range of P_b. For $r_p/\sigma = 50$, on the other hand, the confined phase of intermediate density is never the globally stable one (i.e., it is metastable) and the least dense phase is directly converted into the densest phase, resulting in only one adsorbed phase transition. A similar adsorption profile would also be observed in other two situations: if the adsorption temperature was below a unique critical temperature, or if it was between two critical temperatures.

5. Conclusions

The critical behavior of pure confined fluids predicted by a simple extension of the van der Waals equation of state has been investigated. It was found that this model may predict either one or two mechanically stable critical points for the confined fluid. When two critical points are predicted, one is attributed to a major contribution of molecule–molecule interactions, while the other is attributed to a major contribution of molecule–wall interactions. The confined fluid critical point(s) presented a complex dependence on the pore size, due to the interplay of the molecule–molecule and the molecule–wall interactions. The prediction of two stable critical points results from high values of the energy parameter of the molecule–wall interaction potential and occurs in moderate to large pore sizes. However, as the pore size increases, one of these critical points tends to null density, while the other tends to the bulk critical point. Therefore, only one critical point with physical meaning is predicted for bulk fluids, as expected. It was shown that the prediction of two critical points for confined fluids is useful to describe adsorption isotherms with two phase transitions.

Acknowledgments

L.T. and F.W.T. thank the financial support of CNPq and FAPERJ. M.C. thanks the support of the CAPES/Fulbright program for a Senior Visiting Professor scholarship at the University of Delaware. This research was partially supported by grant number CTS-0083709 from the National Science Foundation.

References

[1] A.P.Y. Wong, S.B. Kim, W.I. Goldburg, M.H.W. Chan, Phase-separation, density fluctuation, and critical-dynamics of N_2 in aerogel, Physical Review Letters 70 (1993) 954–957.
[2] M. Thommes, G.H. Findenegg, M. Schoen, Critical depletion of a pure fluid in controlled-pore glass: experimental results and grand canonical ensemble Monte Carlo simulation, Langmuir 11 (1995) 2137–2142.
[3] Y. Hiejima, M. Yao, Phase behaviour of water confined in Vycor glass at high temperatures and pressures, Journal of Physics: Condensed Matter 16 (2004) 7903–7908.
[4] V.G. Arakcheev, A.A. Valeev, V.B. Morozov, A.N. Olenin, CARS diagnostics of molecular media under nanoporous confinement, Laser Physics 18 (2008) 1451–1458.
[5] M. Thommes, G.H. Findenegg, Pore condensation and critical-point shift of a fluid in controlled-pore glass, Langmuir 10 (1994) 4270–4277.
[6] K. Morishige, M. Shikimi, Adsorption hysteresis and pore critical temperature in a single cylindrical pore, Journal of Chemical Physics 108 (1998) 7821–7824.
[7] A. Vishnyakov, E.M. Piotrovskaya, E.N. Brodskaya, E.V. Votyakov, Y.K. Tovbin, Critical properties of Lennard–Jones fluids in narrow slit-shaped pores, Langmuir 17 (2001) 4451–4458.
[8] H.L. Vortler, Simulation of fluid phase equilibria in square-well fluids: from three to two dimensions, Collection of Czechoslovak Chemical Communications 73 (2008) 518–532.
[9] S. Jana, J.K. Singh, S.K. Kwak, Vapor–liquid critical and interfacial properties of square-well fluids in slit pores, Journal of Chemical Physics 130 (2009), 214707 (1–8).
[10] S.K. Singh, A. Sinha, G. Deo, J.K. Singh, Vapor–liquid phase coexistence, critical properties, and surface tension of confined alkanes, Journal of Physical Chemistry C 113 (2009) 7170–7180.
[11] M. Alvarez, D. Levesque, J.J. Weis, Monte Carlo approach to the gas–liquid transition in porous materials, Physical Review E 60 (1999) 5495–5504.
[12] C. Spöler, S.H.L. Klapp, Phase behavior of Stockmayer fluids confined to a non-polar porous material, Journal of Chemical Physics 118 (2003) 3628–3638.
[13] J. Jiang, S.I. Sandler, Adsorption and phase transitions on nanoporous carbonaceous materials: insights from molecular simulations, Fluid Phase Equilibria 228–229 (2005) 189–195.
[14] V. De Grandis, P. Gallo, M. Rovere, The phase diagram of confined fluids, Journal of Molecular Liquids 134 (2007) 90–93.
[15] X. Zhang, W. Wang, Square-well fluids in confined space with discretely attractive wall-fluid potentials: critical point shift, Physical Review E 74 (2006), 062601 (1–4).

[16] J.K. Singh, S.K. Kwak, Surface tension and vapor–liquid phase coexistence of confined square-well fluid, Journal of Chemical Physics 126 (2007), 024702 (1–8).
[17] T.W. Rosch, J.R. Errington, Phase behavior of model confined fluids: influence of substrate–fluid interaction strength, Journal of Physical Chemistry B 112 (2008) 14911–14919.
[18] M. Schoen, D.J. Diestler, Analytical treatment of a simple fluid adsorbed in a slit-pore, Journal of Chemical Physics 109 (1998) 5596–5606.
[19] A. Giaya, R.W. Thompson, Water confined in cylindrical micropores, Journal of Chemical Physics 117 (2002) 3464–3475.
[20] G.J. Zarragoicoechea, V.A. Kuz, van der Waals equation of state for a fluid in a nanopore, Physical Review E 65 (2002), 021110 (1–4).
[21] A.G. Meyra, G.J. Zarragoicoechea, V.A. Kuz, Thermodynamic equations for a confined fluid at nanometric scale, Fluid Phase Equilibria 230 (2005) 9–14.
[22] E.G. Derouane, On the physical state of molecules in microporous solids, Microporous and Mesoporous Materials 104 (2007) 46–51.
[23] L. Travalloni, M. Castier, F.W. Tavares, S.I. Sandler, Thermodynamic modeling of confined fluids using an extension of the generalized van der Waals theory, Chemical Engineering Science 65 (2010) 3088–3099.
[24] S.I. Sandler, The generalized van der Waals partition function. I. Basic theory, Fluid Phase Equilibria 19 (1985) 233–257.
[25] K.-H. Lee, M. Lombardo, S.I. Sandler, The generalized van der Waals partition function. II. Application to the square-well fluid, Fluid Phase Equilibria 21 (1985) 177–196.
[26] G.E. Mueller, Numerically packing spheres in cylinders, Powder Technology 159 (2005) 105–110.
[27] T.M. Truskett, P.G. Debenedetti, S. Torquato, Thermodynamic implications of confinement for a waterlike fluid, Journal of Chemical Physics 114 (2001) 2401–2418.
[28] G. Franzese, G. Malescio, A. Skibinsky, S.V. Buldyrev, H.E. Stanley, Generic mechanism for generating a liquid–liquid phase transition, Nature 409 (2001) 692–695.
[29] J.W. Tester, M. Modell, Thermodynamics and its Applications, Prentice Hall, New Jersey, 1996.
[30] B.E. Poling, J.M. Prausnitz, J.P. O'Connell, The Properties of Gases and Liquids, McGraw-Hill, New York, 2000.
[31] T.L. Hill, An Introduction to Statistical Thermodynamics, Addison-Wesley, Massachusetts, 1960.